

An improved simulation model for Nakagami- m fading channels for satellite positioning applications

Elina Pajala, Tero Isotalo, Abdelmonaem Lakhzouri, Elena Simona Lohan

Institute of Communications Engineering
Tampere University of Technology
P.O.Box 553, FIN-33101 Tampere, Finland

e-mails: {elina.pajala, tero.isotalo, abdelmonaem.lakhzouri, elena-simona.lohan}@tut.fi

Abstract - This paper presents a simple and efficient simulation model for Nakagami- m fading channels. We first show, via measurement data, that the Nakagami- m distribution provides the best fit for the fading amplitudes of the satellite-to-indoor and satellite-to-outdoor channels. Therefore, finding a viable simulation model for Nakagami- m distribution is very important for the purpose of studying signal and link level positioning algorithms. We then extend a previously proposed method, namely the Beaulieu &al method, to a wider range of m -values, keeping a low computational effort. Theoretical results are validated via comparison with simulation-based curves, and the limits of the algorithm are discussed.

1 Introduction

Nakagami- m distribution has gained a lot of attention lately, due to its ability to model a wider class of fading channel conditions and to fit well the empirical data. However, the simulation models for Nakagami- m distributed fading channels exist in literature only for values of the Nakagami parameter m between 0.5 and 10 [1, 2]. Also, the modelling for $0.5 < m < 0.65$ is typically computationally quite expensive [2]. The simplest model for simulating Nakagami- m fading channels, based on a simplified approximation of the inverse of the cumulative distribution function (CDF) of the Nakagami distribution, was given by Beaulieu &al in [1]. Although the model in [1] is meant to cover arbitrary values for m between 0.65 and 10, only 12 values in this interval are tabulated, and the procedure of obtaining an arbitrary value besides those tabulated is not explicit or straightforward.

The purpose of our paper is twofold: first, based on measurement data, we show that Nakagami- m distribution is very likely to model various satellite channels (indoor and outdoor). Secondly, we present here an efficient method to generate Nakagami- m channel straight from Rayleigh-distributed variables, by using an accurate approximation function. Our method extends the Beaulieu &al method [1] to a wider range of Nakagami m -parameters (i.e., from 0.5 to 16) and has a low computational effort. We explain the steps to be taken when an interpolation-based approach is used in order to obtain arbitrary m -values in the above mentioned interval. We will also show the channel power spectral densities (PSD) if the assumption of uniform-distributed phases is used, and compare the simulations with the measurement data.

The main motivation of our work comes from the fact that only few studies are found in the literature that have attempted to develop channel models specifically for the satellite-to-indoor channels. The first attempt was back to 1997 [3], where the authors used strong reference data to augment indoor processing capabilities and conduct coherent integrations of up to 160 ms. The existence of deep fades and their impact on indoor signals was observed. In [4] and in [5], the authors have evaluated the Karasawa model and urban three-state fade model (UTSFM) as applied to GPS (global positioning system) signals in difficult environments using standard and high-sensitivity GPS receivers. The most recent study was found in [6], where the author analyzed high-bandwidth raw GPS data with high-sensitivity techniques to characterize the fading. Also in [4] and in [5], it has been reported that over a long period of time, the distribution of signal fading appears to have Rayleigh, Rician, and Loo's components dependent on the nature of the presumed LOS (line-of-sight) propagation path. However, no general conclusion was reported.

In some more recent studies [7, 8], measurement campaigns with data from GPS satellites have shown that the satellite-to-indoor and satellite-to-outdoor channels are most likely to obey a Nakagami- m distribution, with m factor varying according to the channel type (e.g., lower for indoor channels than outdoor channels). Moreover, CDMA interference coming from a low number of satellites can be also described via Nakagami- m distribution [9]. Nakagami- m distribution may also be encountered in urban WCDMA channels [10].

The next section presents the theoretical background of Nakagami- m distribution. Section 3 shows an example of GPS fading channel distributions, based on field measurement data, in order to justify the need for Nakagami- m channel simulation models. The fading channel model used in this paper is introduced in Section 4. Section 5 explains the method by Beaulieu & al. In Section 6, our proposed approach is described in detail, and coefficient values for wider range of m -parameter are presented. Finally, the conclusions are drawn in Section 7.

2 Theoretical background

With Nakagami- m distribution [11], sometimes denoted by m -distribution, a wide class of fading channel conditions can be modeled as explained in our introduction. This fading distribution has gained a lot of attention lately, since the Nakagami- m distribution often gives the best fit to land-mobile and indoor mobile multipath propagation as well as scintillating ionospheric radio links [12]. More recent studies also showed that Nakagami- m gives the best fit for satellite-to-indoor and satellite-to-outdoor radio wave propagation [7, 9].

The probability density function (PDF) for a Nakagami- m distributed channel can be expressed as [1, 13, 14]

$$p_R(R) = \frac{2m^m R^{2m-1}}{\Omega^m \Gamma(m)} \exp\left(-\frac{mR^2}{\Omega}\right), \quad (1)$$

where the channel amplitude $R \geq 0$, $\Omega = \mathbf{E}(R^2)$ is average fading power, $\mathbf{E}(\cdot)$ is the expectation operator, and $\Gamma(\cdot)$ is gamma function. Above, m is the Nakagami fading parameter which determines the severity of the fading [12]. m is the inverse of the normalized variance of R^2 :

$$m = \frac{\left(\mathbf{E}(R^2)\right)^2}{\text{Var}(R^2)}, \quad (2)$$

where $\text{Var}(R^2)$ is the variance of R^2 . The value for m ranges between 1/2 and ∞ . When $m \rightarrow \infty$, the channel converges a static channel. [11]

As special cases, Nakagami- m includes Rayleigh distribution when $m = 1$, and one-sided Gaussian distribution for $m = 1/2$. This basically means that, if $m < 1$, the Nakagami- m distributed fading is more severe than Rayleigh fading, and for values of $m > 1$, the fading circumstances are less severe. For the values of $m > 1$, the Nakagami- m distribution closely approximates the Rician distribution, and the parameters m and the Rician factor K (which determines the severity of the Rician fading) can be mapped via the equation of $m = \frac{(1+K)^2}{1+2K}$, when $K \geq 0$. [11]

3 Measurement data

The indoor measurement campaign was carried out with the help of u-Nav Microelectronics on 6th of April, 2004, in Tampere, Finland. Two GPS receivers, synchronized to a common clock, were used. The first one acquires the signal from an outdoor antenna placed on the roof of the building. The second antenna is moving in an indoor environment at pedestrian speed. The signal from the outdoor antenna is expected to be strong, and it will be used as reference signal for code phase and Doppler frequency acquisition, as well as for navigation data estimation [7, 8, 9]. Both receivers are using a sampling rate of 16.36 MHz. Each measurement has a duration of 2 mn, which gives about 1956 M samples per satellite and per scenario and is considered to be sufficient for reliable statistical characterization.

3.1 Data Processing

The signal at the GPS receiver can be written as [15]:

$$r(t) = \sum_{s=1}^{N_{sv}} d_s(t - \tau_s) \beta_s(t - \tau_s) e^{+j2\pi f_{D_s} t} C_s(t - \tau_s) + \eta(t), \quad (3)$$

where t is the GPS time, N_{sv} is the number of satellites in view at time t and $d_s(\cdot)$ is the data bit from satellite s . The complex channel coefficient, instantaneous delay, and Doppler frequency from satellite s at time t are defined respectively by $\beta_s(t)$, τ_s , and f_{D_s} . Here $C_s(t)$ is the transmitted code and $\eta(t)$ is an additive noise.

The output of the correlator corresponding to the satellite v , to the tentative delay τ , and to the Doppler frequency f_D is:

$$y_v(\tau, f_D) = \frac{1}{T} \int_T r(t) e^{-j2\pi f_D t} C_v^{(r)}(t - \tau) dt, \quad (4)$$

where T is the coherent integration time and $C_v^{(r)}(\cdot)$ is the replica of the PRN code at the receiver. The integration time T can be defined as $T = T_c \times S_F \times N_c$, where T_c is the chip interval, $T_c = 1/f_c$, S_F is the code epoch length or the spreading factor, and N_c is the number of coherently combined code epochs. For GPS L1 C/A signal, $f_c = 1.023$ MHz and $S_F = 1023$. The distribution of the signal amplitude $R = |\beta_s|$ was compared to different theoretical distributions such as Rayleigh, Rician, Nakagami. The PDF of a Nakagami- m fading channel coefficient with amplitude R is given by Eq. (1) and the Nakagami- m parameter is given by Eq. (2).

3.2 Measurement-based fading distributions

In what follows, we check the fitting of the indoor and outdoor signal amplitude distributions to Rayleigh, Rice, and Nakagami- m distributions. The m factor in Nakagami- m distribution is estimated from the measurement data, via Eq. (2). As we can see in Fig. 1, both indoor and outdoor signal amplitudes have a clear fitting to the Nakagami- m distribution. We can also notice that in outdoor propagation, the signal amplitude distribution has quite strong m factor as shown in Fig. 1(a).

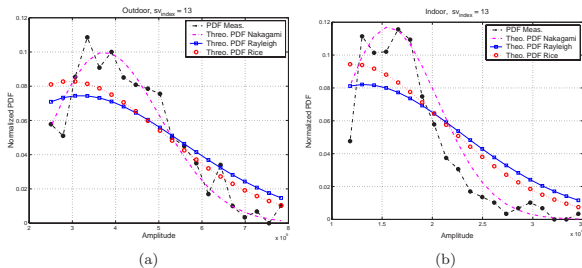


Figure 1: Outdoor and indoor amplitude distribution fitting, Sat=13, $N_c = 200$ ms. (a) Outdoor signal, $m = 5.54$. (b) Indoor signal, $m = 2.33$.

In Fig. 2 we show the Doppler spectrum of both indoor and outdoor signals. The goal was to model the Doppler spectrum by well known power spectrum such as Clarke, asymmetric Clarke or Laplacian power spectra. The Doppler spectrum drawn in Fig. 2 shows that there is only one peak in the range of frequency $[-500, 500]$ Hz, which is the bandwidth at the time domain correlation output. Therefore, it is not straightforward to model the power spectrum using Clarke model. Moreover, the lobe of the main peak is symmetric which indicates that the power spectrum can not be modeled using Laplacian either.

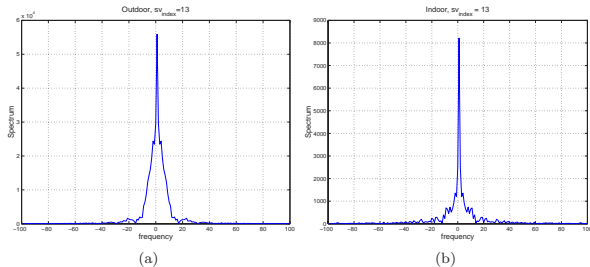


Figure 2: Spectrum of both (a) outdoor and (b) indoor signals. Sat=13, $N_c = 200$ ms.

4 Simulation model

The fading channel model used in this paper is based on the multiple input multiple output (MIMO) radio channel model of Schumacher & al [16, 17, 18], where the transmitted signal is affected by multipath fading channel environment via specific channel coefficients. The coefficients are generated in frequency domain in order to achieve speed-dependent spectrum. Since MIMO modelling is not necessary from the point of view of this paper, the MIMO model of [16, 17, 18] is simplified to single input single output (SISO) channel model.

Fig. 3 presents the simple block diagram of the generation of the fading channel coefficients via the channel model described in [17, 18]. $S(f)$ is the Doppler spectrum, which is here chosen according to Clarke model. Clarke spectrum is usually valid when the phases of the multipaths arriving at the receiver are uniformly distributed in $[0, 2\pi]$. The channel coefficients in the above model can be chosen to be either Rician or Rayleigh-distributed. In the next section we will explain how to extend this model to Nakagami- m distributions.

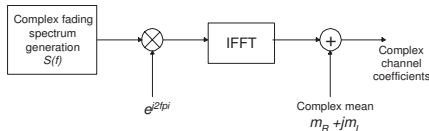


Figure 3: Block diagram of the generation of the fading channel coefficients.

5 Beaulieu & al method

In [1], it was shown that Nakagami- m distributed fading channel parameters can be generated straight from Rayleigh distributed random variables using certain transforms. The basic idea is illustrated in Fig. 4, without the supplementary interpolation stage (dashed block and lines). Rayleigh distributed amplitudes from the channel model of Schumacher & al are transformed to Nakagami- m distributed by Beaulieu's functions. The phases are assumed to remain uniformly distributed, assumption which was explained to be quite reasonable for a wide range of wireless channels [1].

Beaulieu & al method is based on the accurate approximation for the inverse of Nakagami- m CDF. The inverse CDF function $F_R(\cdot)$ for Nakagami- m fading can be expressed as

$$F_R(x) = \int_0^x \frac{2m^m t^{2m-1}}{\Omega^m \Gamma(m)} \exp\left(-\frac{mt^2}{\Omega}\right) dt. \quad (5)$$

where R is a random variable and

$$u = 1 - e^{-R^2/2\sigma^2}. \quad (6)$$

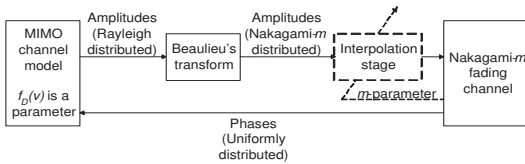


Figure 4: Implementing Beaulieu's transforms for Schumacher's channel model. Dashed block of the interpolation stage is only in the proposed approach.

σ^2 is the second moment of random variable R (i.e., $\sigma^2 = E[R^2]$). [1]

Since the inverse function can not be directly generated, Beaulieu & al proposed the following approximation $F_R^{-1}(u) \approx G(\eta(u))$, where

$$G(\eta(u)) = \eta(u) + \frac{a_1\eta(u) + a_2\eta(u)^2 + a_3\eta(u)^3}{1 + b_1\eta(u) + b_2\eta(u)^2}. \quad (7)$$

Here, $\eta(u)$ is defined as

$$\eta(u) = \left(\sqrt{ln \frac{1}{1-u}} \right)^{\frac{1}{m}}. \quad (8)$$

Above, a_1 , a_2 , a_3 , b_1 , and b_2 are the coefficients which minimize the approximation error $\sum_{u \in (0,1)} \left| F_R^{-1}(u) - G(\eta(u)) \right|^2$. These coefficients are dependent on m and some examples of them can be seen in Table I of [1]. The coefficients for other values than those given in [1] can be also obtained by minimizing the above approximation error, at the expense of large computational effort. [1]

6 Proposed approach

Since Beaulieu & al presented the coefficients selected to minimize the approximation error only for finite values of m between 0.65 and 10, the target of this paper is to extend the method proposed by Beaulieu & al for a wider range of m -values via lower computational effort. The block diagram for the Nakagami- m channel model is that one of Fig. 4, with the supplementary interpolation stage (dashed block and lines). The coefficients already defined by Beaulieu & al are kept as such (see [1]). The rest of the coefficients are chosen according to the minimum error between the theoretical and simulated Nakagami- m distributed PDFs, and to the minimum error between the target m and the true m , as it will be explained here.

The generation of the coefficients was divided into three parts: extrapolation for $0.50 \leq m < 0.65$, interpolation for $0.65 \leq m \leq 10$ (i.e., for those m -values which were not presented in [1]), and extrapolation for $m > 10$.

The generation of the coefficients for $0.65 \leq m \leq 10$, in-between the coefficient values presented in [1], turned out to be rather simple with only linear interpolation. The extrapolation of the coefficients for $0.5 \leq m < 1$ and $m > 10$ was noticed to be more complex. Both linear and n -th order polynomial extrapolation were tried, with values of n between 1 and 3. No accurate match either to linear or to polynomial extrapolation was found, but the correct coefficient values were noticed to be situated between the results of linear and 2nd order polynomial extrapolation, or to the close approximate of those. Thus, the linear and 2nd order polynomial extrapolation curves defined the limits for the search process, and the correct coefficient values were searched between and nearby of the curves. This is illustrated in Fig. 5, which shows an example of the simulated coefficient values together with the linear interpolation and both linear and 2nd order polynomial extrapolation for coefficient a_3 .

The coefficients were chosen according to two conditions: the error between the theoretical and simulated Nakagami- m distributed PDFs (J_1), and the error between the target m and the true m of the channel (J_2):

$$J_1 = \sum_{R=0}^{\infty} |p_{sim}(R, \underline{\alpha}) - p_{th}(R)|^2, \quad (9)$$

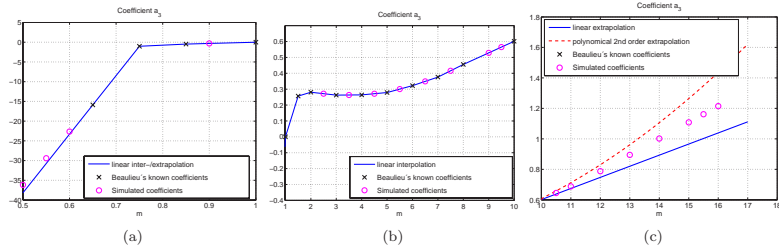


Figure 5: An example of linearly interpolated and both linearly and polynomially (2nd order) extrapolated coefficient values for a_3 with the simulated and known coefficient values. (a) Extrapolation and interpolation for $0.5 \leq m < 1$. (b) Interpolation for $1 \leq m \leq 10$. (c) Extrapolation for $m > 10$. Similar plots are obtained for the rest of a_i and b_k coefficients, $i = 1, 3$, $k = 1, 2$.

where $\underline{\alpha} = [a_1 \ a_2 \ a_3 \ b_1 \ b_2]$ are the coefficients in test, $p_{sim}(R, \underline{\alpha})$ is the simulated PDF for the coefficients $\underline{\alpha}$, and $p_{th}(R)$ is the theoretical PDF.

$$J_2 = |m_{sim}(\underline{\alpha}) - m_{th}|^2, \quad (10)$$

where $m_{sim}(\underline{\alpha})$ is the true m of the simulated channel, and m_{th} is the target m , i.e., m of the theoretical PDF. The best coefficients $\hat{\underline{\alpha}}$ were chosen to be those coefficients, which minimize $J_1 + J_2$ criterion:

$$\hat{\underline{\alpha}} = \underset{\underline{\alpha}}{\operatorname{argmin}} (J_1 + J_2). \quad (11)$$

As it can be seen in Fig. 5(c), the lines resulted from the linear and polynomial interpolations are separating when the value of m increases. This leads to a wider uncertainty region and thus, to increasing number of coefficient alternatives to be tested. In practice, the coefficients for wider range of m were searched iteratively, e.g., at first looking for the coefficients for $m = 11$, and then performing the linear and polynomial extrapolations again taking account the coefficient values for $m = 11$, so that the coefficients for $m = 12$ could be more easily defined. As m increased, the computation time required to find correct coefficients was increasing as well, and, for $m > 16$, finding the correct coefficients with the proposed method turned out to be rather difficult in a reasonable time. On the other hand, as can be seen in Fig. 6, the shape of the PDF for $m = 17$ starts to be similar to the PDF of a single-path static channel (i.e., one single peak when $m \rightarrow \infty$). However, this kind of shape of the PDF may also result for lower values of m , in the case of incorrect approximation coefficients.

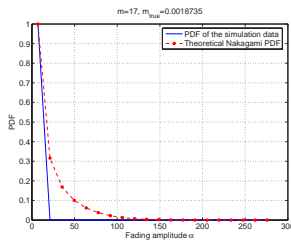


Figure 6: Example of failed matching between the theoretical and simulated Nakagami- m PDF. $m = 17$.

Some illustrative values of the generated coefficients for Beaulieu's transforms are shown in Fig. 7 and in Table 1. Not all the generated values are presented, due to the lack of space, but the coefficient values for $0.5 \leq m \leq 16$ can be approximated quite well via linear interpolation using the coefficient values presented in [1] and in Table 1 here.

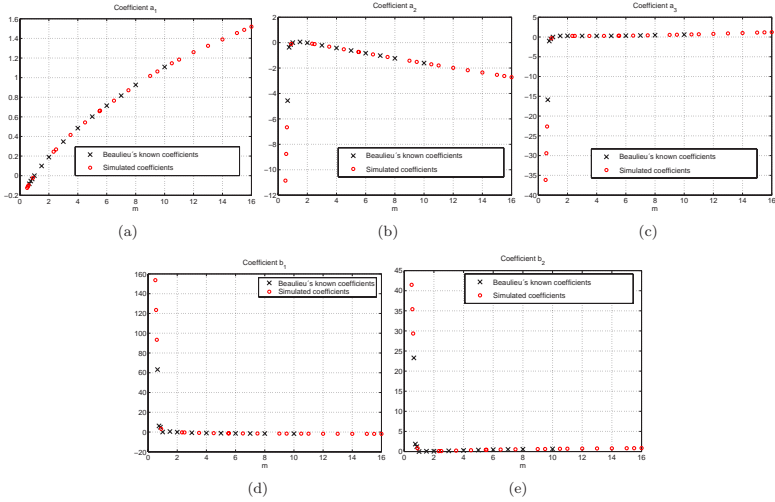


Figure 7: Examples of simulated and known coefficients for: (a) coefficient a_1 , (b) coefficient a_2 , (c) coefficient a_3 , (d) coefficient b_1 , and (e) coefficient b_2 .

m	a_1	a_2	a_3	b_1	b_2
0.50	-0.1250	-10.8567	-36.1544	153.6727	41.4653
0.55	-0.1109	-8.7589	-29.3969	123.5136	35.4096
0.60	-0.0969	-6.6612	-22.6394	93.3546	29.3539
0.90	-0.0224	-0.1029	-0.3155	3.2833	0.8055
2.33	0.2444	-0.0834	0.2744	-0.2899	0.1006
2.5	0.2681	-0.1137	0.2717	-0.3794	0.1164
3.5	0.4159	-0.3188	0.2634	-0.8254	0.2208
5.54	0.6637	-0.7375	0.3028	-1.2587	0.4186
9.0	1.0174	-1.4223	0.5286	-1.5459	0.6058
9.5	1.0631	-1.5159	0.5651	-1.5753	0.6273
10.5	1.1464	-1.7039	0.6449	-1.6344	0.6722
11.0	1.1839	-1.7983	0.6883	-1.6642	0.6955
11.5	1.2218	-1.8921	0.7380	-1.6869	0.7148
12.0	1.2596	-1.9859	0.7878	-1.7096	0.7340
13.0	1.3247	-2.1692	0.8949	-1.7408	0.7608
14.0	1.3898	-2.3526	1.0020	-1.7719	0.7875
15.0	1.4550	-2.5349	1.1083	-1.8082	0.8194
15.5	1.4874	-2.6264	1.1615	-1.8264	0.8353
16.0	1.5197	-2.7178	1.2147	-1.8446	0.8512

Table 1: Illustrative examples of the simulated values for coefficients a_1 , a_2 , a_3 , b_1 , and b_2

In Fig. 8, the PDFs of theoretical (dashed and dotted red line) and simulated (solid blue line) Nakagami- m distributed fading amplitudes are shown with good matching. PDFs for all presented values match similarly to theoretical values; there is typically a slight mismatch, which also varies by the simulation round since a finite number of random variables is generated.

Fig. 9 shows the channel PSD for $m = 5.54$ and for $m = 2.33$, with a terminal speed of 1 km/h. When comparing the simulated PSD with the PSD obtained via measurements (Fig. 2), we can see that the simulated channel match well with the measurement data, and, thus, the assumption of uniformly distributed phases hold.

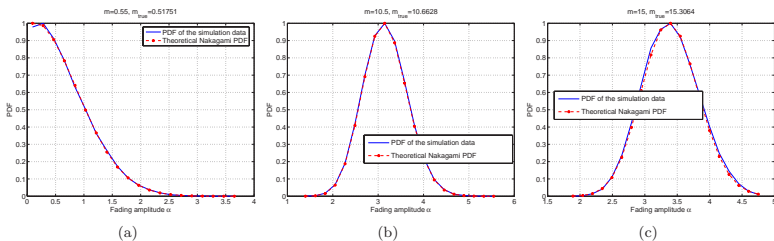


Figure 8: Examples of simulated and theoretical Nakagami- m PDFs for selected values of m : (a) $m = 0.55$, (b) $m = 10.5$, and (c) $m = 15$. m is the target m -value and m_{true} is the true m -value for the simulated channel.

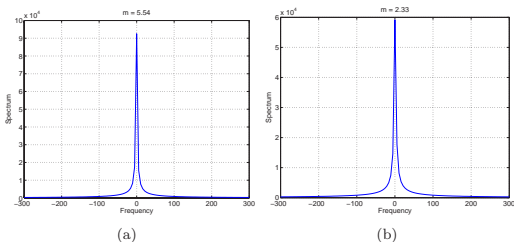


Figure 9: Power Spectral Density for simulated channel: (a) $m = 5.54$ and (b) $m = 2.33$. $N_c = 200$ ms.

7 Conclusions

Simulation models for Nakagami- m distributed fading channels exist in literature only for m -values between 0.5 and 10. One of the simplest methods has been proposed by Beaulieu & al. In their method, the Nakagami- m channel is generated straight from Rayleigh distributed variables using an accurate approximation function for the inverse of the CDF of the Nakagami distribution. In this paper, we have presented a simple and efficient simulation model for Nakagami- m fading channels, by extending the method proposed by Beaulieu & al to a wider range of m -values. The extended model has low computational effort and it has been described in detail in our paper. The approximation coefficients are presented for m -parameter from 0.5 to 16, and the PDFs for simulated and theoretical Nakagami- m channels are compared. Based on measurement data from GPS satellites, we have shown that the Nakagami- m distribution provides the best fit for the fading amplitudes, for both indoor and outdoor channels. We have also shown, that the PSD of the simulated Nakagami- m channel is matching well with the PSD of the measurement data.

References

- [1] N. C. Beaulieu and C. Cheng. An Efficient Procedure for Nakagami-m Fading Simulation. In *IEEE Proc. of Globecom 2001*, volume 6, pages 3336–3342, Nov 2001.
- [2] K. W. Yip and T. S. Ng. A simulation model for nakagami-m fading channels, $m < 1$. *IEEE Transactions on Communications*, 48(2):214–221, Feb 2000.
- [3] B. Peterson, D. Bruckner, and S. Heye. Measuring GPS signals indoors. In *Proc. of ION GPS*, pages 615–624, Sep 1997.
- [4] R. Klukas, G. Lachapelle, C. Ma, and G.I. Jee. GPS signal fading model for urban centres. *IEE Proceedings on Microwaves, Antennas and Propagation*, pages 245–252, 2003.
- [5] C. Ma, G. Jee, G. MacGougan, G. Lachapelle, S. Bloebaum, G. Cox, L. Garin, and J. Shewfelt. GPS signal degradation modeling. In *Proc. of ION GPS*, pages 882–893, Sep 2001.
- [6] John Robert Watson. High-sensitivity GPS L1 signal analysis for indoor channel modelling. Master's thesis, Department of Geomatics Engineering, University of Calgary, Alberta, Canada, Apr 2005.
- [7] A. Lakhzouri, E. S. Lohan, I. Saastamoinen, and M. Renfors. Measurement and Characterization of Satellite-to-Indoor Radio Wave Propagation Channel. In *CDROM Proc. of The European Navigation Conference (ENC-GNSS '05)*, Munich, Germany, Jul 2005.
- [8] A. Lakhzouri, E. S. Lohan, I. Saastamoinen, and M Renfors. On second order statistics of the satellite-to-indoor channel based on field measurements. In *CDROM Proc. of PIMRC*, Sep 2005.
- [9] A. Lakhzouri, E. S. Lohan, I. Saastamoinen, and M. Renfors. Interference and Indoor Channel Propagation Modeling Based on GPS Satellite Signal Measurements. In *Proc. of ION GPS*, pages 896–901, Sep 2005.
- [10] E. S. Lohan, A. Lakhzouri, and M. Renfors. Statistical Properties of Urban WCDMA Channel for Mobile Positioning Applications. *International Journal of Wireless and Optical Communications (IJWOC)*, 2(2), Dec 2004.
- [11] M. Nakagami. The m -distribution - A General Formula of Intensity Distribution of Rapid Fading. In *W. C. Hoffman: Statistical Methods of Radio Wave Propagation*, Oxford, England, 1960.
- [12] M.K. Simon, J.K. Omura, R.A. Scholtz, and B.K. Levitt. *Spread Spectrum Communication Handbook*. McGraw-Hill Inc, New York, revised edition edition, 1994.
- [13] A.F. Abouraddy and S.M. Elnoubi. Statistical Modelling of the Indoor Radio Channel at 10 GHz through Propagation Measurements - Part 1: Narrow-band Measurements and Modelling. *IEEE Trans. on Vehicular Technology*, 49(5):1491–1507, Sep 2000.
- [14] M.K. Simon and M.S. Alouini. *Digital Communications over Fading Channels: A Unified Approach to Performance Analysis*. Wiley InterScience, Sep 2000.
- [15] E.D. Kaplan. *Understanding GPS, Principles and applications*. Artech House, Boston, 1996.
- [16] L. Schumacher, J. P. Keramoal, F. Frederiksen, K. I. Pedersen, A. Algans, and P. Mogensen. *MIMO Channel Characterisation*. IST Project IST-1999-11729 METRA Deliverable D2, Feb 2001.
- [17] K.I. Pedersen, J. B. Andersen, J. P. Keramoal, and P. Mogensen. A stochastic multiple-input-multiple-output radio channel model for evaluation of space-time coding algorithms. In *Proc. of IEEE VTC Fall*, volume 2, pages 893–897, Boston, USA, Sep 2000.
- [18] L. Schumacher, K. I. Pedersen, and P. E. Mogensen. From antenna spacings to theoretical capacities - guidelines for simulating MIMO systems. In *13th IEEE International Symposium on Personal, Indoor and Mobile Radio Communications*, volume 2, pages 587–592, Sep 2002.

